

H α polarimetry of the solar limb

D. Clarke and V. Ameijenda

University Observatory, Acre Road, Glasgow, G20 0TL, Scotland, UK (d.clarke@astro.gla.ac.uk)

Received 6 September 1999 / Accepted 21 January 2000

Abstract. A prototype H α imaging polarimeter has been used to make measurements of the solar disk. Within the H α line, the polarization at the solar limb is significantly greater than the nearby continuum reflecting resonance scattering effects, with p achieving $\sim 0.3\%$ at the line-core. Comparative measurements have been made of the form of polar and equatorial center-to-limb variations (CLVs). Face value results indicate that the polarization emanating from the pole is marginally greater than from the equator. This finding is explainable, however, in terms of instrumental, experimental and data reduction effects with the conclusion that no disparity between the polar and equatorial p -CLVs has been detected to polarimetric accuracies $\sim \pm 0.02\%$ or 2 parts in 10^4 and to a spatial accuracy ~ 1 arcsec. Some of the recorded CLVs show departures from a smooth curve, these associated with magnetic structures and the Hanle effect.

Key words: polarization – scattering – instrumentation: polarimeters – techniques: polarimetric – Sun: chromosphere – Sun: photosphere

1. Introduction

Polarimetry plays an important role as a diagnostic for many physical processes occurring in the solar photosphere and chromosphere. Observational and theoretical investigations of polarimetric structures within a variety of Fraunhofer lines have recently expanded to a level that such spectropolarimetry is now referred to as the study of the “second” solar spectrum (see Stenflo, 1996 and Stenflo and Keller, 1997). Solar polarimetry involves either the measurement of the spectral variation of the degree of polarization, $p(\lambda)$, at selected locations on the solar disk or the investigation of p across surface structures, with measurements made at a particular wavelength. The latter includes measurements of the center-to-limb variation (CLV) of p explored at a variety of selected wavelengths – see, for example, Leroy (1972), Dollfus (1974) and Mickey and Orrall (1974) – with results which are accurately explained by models such as those by Dumont and Pecker (1971). For the UV passband

used Leroy (1972), it was reported that differences might exist between the p -CLV gradients for equatorial and polar zones, with the solar equator exhibiting marginally higher values of p .

All of this pioneering work on p -CLV studies was undertaken using photomultiplier detectors with the requirement of sequential measurements at calibrated distances along the solar radius. Since then, 2D detectors, such as CCDs, have become available allowing many spatially resolved elements to be monitored simultaneously. This paper describes a simple imaging instrument for mapping linear polarization, working at H α with a passband of 0.4\AA , designed chiefly with the aim of exploring the p -CLV variations within the core of this line and in its wings. Experiments have been undertaken to see if there are differences at H α of the p -CLVs between the solar equator and the poles. Perhaps relevant to such studies are the recent H α photometric measurements of Auchère et al. (1998) revealing that the solar chromosphere appears prolate ($\Delta D/D = 1.2 \times 10^{-3}$) in this spectral line. If this effect is related to differences in the behaviour of the optical depth or limb darkening between equatorial and polar radial sections, then it is also likely that there will be differences in the p -CLV between the solar equator and the poles.

The instrument has also been used to explore the Hanle effect in H α across surface features where magnetic fields are present and to map the polarization structures of prominences.

2. The instrument

The overall instrument comprised a 250 mm (f/10) Meade telescope incorporating a narrow-band H α filter system operating in a converted f/32 beam. The passband of the filter (Daystar – University Model) was adjustable over a range of $\pm 0.3\text{\AA}$ by altering the temperature of its thermostated enclosure. The polarimeter was attached to this arrangement with the final polarimetric encoded images recorded by an SBIG ST6 CCD camera under PC control. The monochromator system also required a broad-band red dye colour filter, mounted in a cap and placed over the end of the telescope, reducing the effective aperture to about 100mm. Also, because of this, the fore-optics provided an off-axis system with an instrumental polarization affecting all measurements. The way this problem was addressed is described later below.

The imaging polarimetric system was a variation of a design first used by Pickering (1873) and later improved by Öhman (1939). Similar instruments have also been constructed for producing polarization maps of reflection nebulae and galaxies [see, for example, Scarrott (1983, 1991)]. For our design, a rectangular slotted mask (20 mm \times 15 mm) of black dielectric material (Delrin), to avoid spurious edge polarizing effects being introduced (see Pospergelis, 1965) was located at the telescope's focus containing the solar monochromatic image. This piece had rulings 1 mm wide and 14 mm long cut out, with mark-to-space ratio of unity, blocking off five alternate strips, so providing a usable size of 10 mm \times 14 mm, corresponding to a field of view of $8' \times 10'$. A field lens immediately followed the grid to focus the telescope's aperture on a rotatable quartz/MgF₂ superachromatic half-wave plate (manufactured by Halle, Berlin) prior to a 20 mm long calcite Savart prism with 20 mm cross-section. Although such wave plates may give rise to fringes exhibiting low levels of polarization, no spurious signals have been detected with its use here and within previous polarimeters (see Clarke and Fullerton, 1996, for example). The Savart polarizer separated the orthogonally resolved beams, giving them identical displacements with opposite sense. The device provided identical optical path lengths for the two beams so that for a given transparent slot in the grid, two image strips with orthogonal polarizations were focussed side by side in the same plane on the detector. Although Savart plates suffer from astigmatism, this was of no consequence here as the focal ratio of the transmitted beam was large ($f/32$).

The Savart plate was oriented such that the two emerging beams were displaced perpendicularly to the bars of the grid. The telescope focal plane containing the grid was re-imaged on the CCD detector using a 28–80 mm focal length telephoto camera lens. The orientation of the CCD camera was carefully set so that the grid structure was parallel to the pixel columns. With this arrangement, the resolution of each CCD pixel corresponded to $\sim 4''$ on the sky, sufficient for the CLV experiment and not out of keeping with the local seeing conditions. After preliminary experience, a neutral density filter was added prior to the CCD, not affecting the instrumental polarization, to provide manageable exposure times, typically 1 s to 3 s, without pixel saturation.

To provide mechanical stability of the instrument and to allow accurate tracking, the complete system was attached to a metal plate and fixed to the 510 mm telescope at the Cochno site of the University of Glasgow Observatory.

3. Data acquisition and reduction

By employing a double-beam system, the effects of variations in the transparency of the Earth's atmosphere during acquisition of the necessary frames were removed by taking ratios of the orthogonal signals. By taking further ratios corresponding to different settings of the waveplate, self-calibration of the pixel sensitivities was achieved without the need of flat-fielding exercises which are common for CCD photometry. The principle of the scheme has been summarised by Tinbergen (1996) and

the method has also been employed for solar measurements by Bianda et al. (1998a, 1998b). The effectiveness of the design may be appreciated by considering the form of the recorded signals.

For a half-waveplate placed before a fixed polarizer, the modulation of any linear polarized light it accepts is at four times the rate of rotation of the waveplate (see, for example, Clarke and Grainger, 1971). Thus the signals from the double-beam polarimeter can be represented by

$$\begin{aligned} I_{\perp} &= \frac{1}{2}T(t)G_{\perp}(I + Q \cos 4\psi + U \sin 4\psi) \\ I_{\parallel} &= \frac{1}{2}T(t)G_{\parallel}(I - Q \cos 4\psi - U \sin 4\psi) \end{aligned} \quad (1)$$

where the subscripts \perp and \parallel refer to the orthogonally resolved beams, $T(t)$ describes the atmospheric transparency during the time of any exposure, G is the response to unit intensity of a given pixel corresponding to a particular image point; I, Q, U are the Stokes parameters describing the intensity and linear polarization of the light and ψ is the setting of the axis of the waveplate relative to the principal axis of the polarizer.

In order to determine the normalised Stokes parameters, four exposures are taken at settings of the waveplate in multiples of 22.5° . Consider the data reduction for frames with the setting of ψ at 0° and 45° . From Eqs. (1) above, the ratios of matching image pixels are given by

$$R_{0^\circ} = \frac{\frac{1}{2}T_{0^\circ}(t)G_{\parallel}(I + Q)}{\frac{1}{2}T_{0^\circ}(t)G_{\perp}(I - Q)} = \frac{G_{\parallel}(I + Q)}{G_{\perp}(I - Q)} \quad (2)$$

and

$$R_{45^\circ} = \frac{\frac{1}{2}T_{45^\circ}(t)G_{\parallel}(I - Q)}{\frac{1}{2}T_{45^\circ}(t)G_{\perp}(I + Q)} = \frac{G_{\parallel}(I - Q)}{G_{\perp}(I + Q)} \quad (3)$$

Thus the effects of variable atmospheric transmission are removed. The problems of differences in pixel sensitivity are eliminated by taking a further ratio of Eqs. (2) and (3). Thus

$$R_q = \frac{R_{0^\circ}}{R_{45^\circ}} = \frac{\frac{G_{\parallel}(I+Q)}{G_{\perp}(I-Q)}}{\frac{G_{\parallel}(I-Q)}{G_{\perp}(I+Q)}} = \left(\frac{I+Q}{I-Q}\right)^2 \quad (4)$$

from which the normalised Stokes parameter may be calculated as

$$q = \frac{\sqrt{R_q} - 1}{\sqrt{R_q} + 1} \quad (5)$$

Similarly, by using waveplate settings of 22.5° and 112.5° , values for the u parameter can be determined from

$$u = \frac{1 - \sqrt{R_u}}{1 + \sqrt{R_u}} \quad (6)$$

where

$$R_u = \frac{R_{67.5^\circ}}{R_{112.5^\circ}} = \left(\frac{1+U}{1-U}\right)^2$$

The images collected by the data acquisition PC were transferred via disks to UNIX-based workstations. Raw data files

were archived in the standard FITS format. Conversion of files to an NDF format allowed manipulation by the *Starlink* environment. The utilised packages were a combination of KAPPA, GAIA, DAOPHOT, PHOTOM and FIGARO with several C-shell scripts written to automate the data reduction. A further non-Starlink package, IDL, was employed to analyse the data with specific routines not available elsewhere.

In order to complete the data reduction, it was necessary to consider the instrumental polarization and also to translate any measurements from the instrumental frame to the more standard one of celestial equatorial co-ordinates.

To remove the instrumental polarization which, because of the design of the monochromator system, was inevitably high (a few%), two approaches were considered. One involved the construction of a monochromatic depolarizer as suggested by Billings (1951). This was done using two large diameter mica waveplates, one a quarter-waveplate, the other a half-waveplate, the second rotating at twice the speed of the first, the whole assembly placed before the telescope collection aperture. Over any frame exposure, it may be assumed that the subsequent optical system would be receiving randomised polarization averaging to the equivalent of being unpolarized. Details of the design and the device's performance can be found in Ameijenda (1998). The second approach considered that the radiation from the central zone of the Sun was unpolarized. If the observed patch of photosphere is undisturbed with no activity, then symmetry suggests that this would maintain. Day to day repeated observations were made of this solar region and the stability of the result suggested that the recorded values were essentially those of the instrumental polarization. As with the usual practice of stellar polarimetry, the instrumental polarization was subtracted vectorially from the main measurements of the study.

By design, the overall instrument was constructed so that its polarimetric reference frame was set at a 45° position to the N/S direction in equatorial co-ordinates. This was checked out and confirmed by suspending a large piece of polaroid on a plumb line so that exposures could be made with accepted direction of polarization rotated between two angular positions about the vertical direction. For observations made at the meridian passage, the bisector of the pair of recorded position angles corresponds to the N/S direction. A similar arrangement was used by Clarke and Fullerton (1996) in their investigations of global solar polarization.

4. Observations

Fig. 1 encapsulates the measurement scheme for the solar p -CLV investigations. It displays an H α full solar disk image recorded at the Observatoire de Paris. Superimposed on the projected Northern and Western limbs are rectangles corresponding to the sequential placements of one of mask's slits within the focal plane of the telescope. The upper part of the figure displays the records of frames taken by the Glasgow polarimeter, showing the orthogonal polarization pairs of a single slit; there is slight overlap of these images and the pixels from this part of the frame were not included in the data analysis.

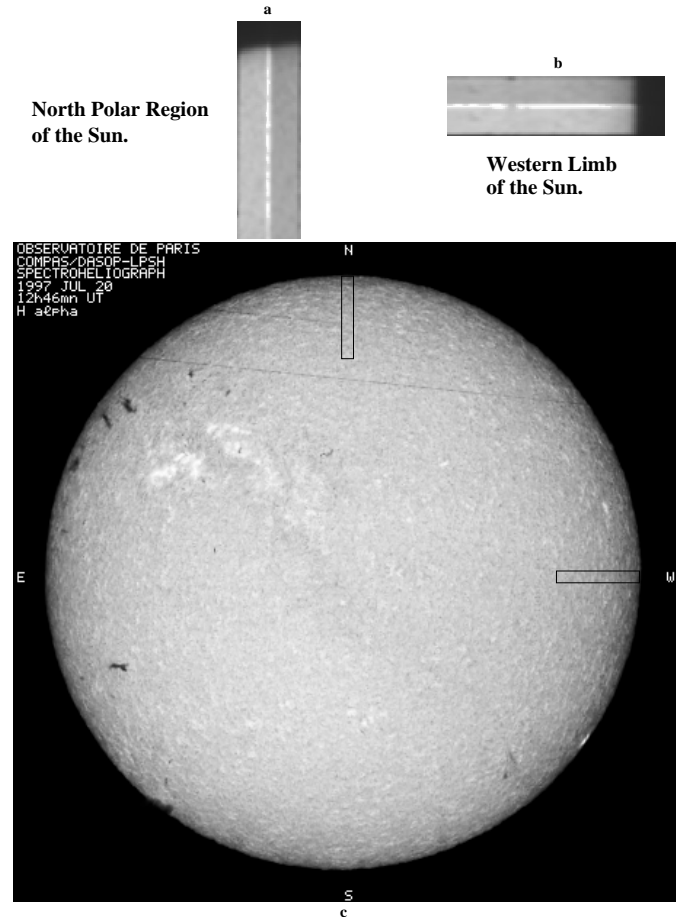


Fig. 1a – c. A visual summary for the p -CLV measurements made on 1997 July 20. The upper sections (a and b) show the orthogonal polarization image pairs from one of the slits with the grid placed parallel to the radial directions on the North and West limbs, as indicated on the full H α solar disk picture c obtained from the Observatoire de Paris.

Four frames corresponding to the half-waveplate orientations $\psi = 0^\circ, 45^\circ, 67.5^\circ$ and 112.5° were taken for complete polarimetric determinations.

An example of the behaviour of the combined basic signals from the pairs of slit images is depicted in Fig. 2 corresponding to a frame taken of the projected Northern pole limb, with the half-waveplate orientation set at $\psi = 0^\circ$. It will be noted that the intensity levels of the orthogonal polarizations, expressed as numbers of recorded photons, are well separated, indicating a relatively high level of polarization, part being instrumentally generated. Away from the limb, it will also be noted that there are correlated intensity variations within the orthogonal signals, these corresponding to structures that could be clearly seen by eye on the solar disk at the time of the observations.

Fully reduced normalised Stokes parameter values, q and u , are plotted against distance within the solar limb in Fig. 3, the error bars indicating the 1σ uncertainties of the measurements as determined from the combination of pixels across the slit width at the given distance from the solar limb. Considering the u parameter first, it can be seen that the mean value is close to

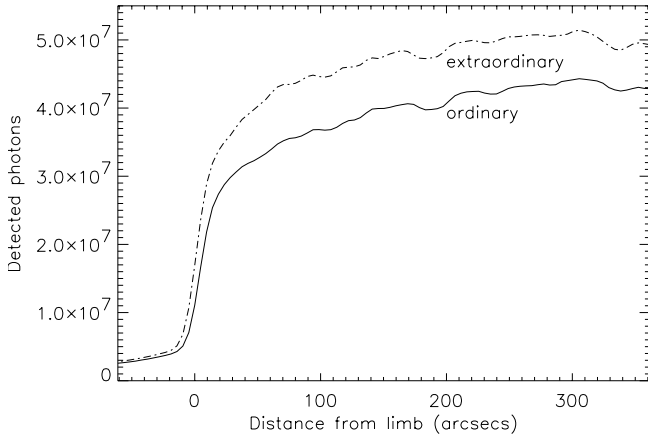


Fig. 2. A record taken on 1997 July 19 of the center-to-limb intensity variation with the half-waveplate orientation set at $\psi = 0^\circ$ for the northern limb. The monochromator was tuned for the core of H α . Note that the orthogonal polarizations (marked ordinary and extraordinary) display correlated structures corresponding to the mottling that is very apparent in solar H α images. The separation of the two curves indicates the presence of a polarimetric signal, including the instrumental effect.

Table 1. Values of the degree of polarization in the core of H α at the heliographic North pole at limb distances of $\mu = 0.1, 0.15$ and 0.20 for observations made in Glasgow and by Stenflo's group.

p -ratio	Glasgow	Stenflo
$p(\mu_{0.10})/p(\mu_{0.15})$	$0.313/0.162 = 1.93$	$0.299/0.148 = 2.02$
$p(\mu_{0.15})/p(\mu_{0.20})$	$0.162/0.084 = 1.94$	$0.148/0.075 = 1.97$
$p(\mu_{0.10})/p(\mu_{0.20})$	$0.313/0.084 = 3.73$	$0.299/0.075 = 3.99$

zero. Thus the degree of polarization is essentially carried by the value of q , indicating that the axes of the polarimeter have been correctly set to be on a projected solar radius along the celestial N/S direction.

According to Fig. 3, $p \sim 0.3\%$ at the limb, falling to 0.1% at $20''$ inside the limb and falling further to background levels at about $40''$ or $\mu \sim 0.3$, so offering ~ 10 data points for the fitting of coefficients to a p -CLV curve.

Based on broadband measurements of Dollfus (1974) at 6000\AA , the recorded polarization here within the core of H α is $10\times$ larger than at its nearby continuum, such an enhancement being typical of the effects of resonant scattering (see Stenflo and Keller, 1997).

From the data recorded on 1997 July 9, H α core values of p (in units of%) at $\mu = 0.1, 0.15$ and 0.20 have been abstracted to allow comparison with measurements by Stenflo et al. (1997) and Keller (1998) at the heliographic North pole, made in 1994 November (see Table 1).

It may be noted that the Glasgow measurements carry uncertainties on $p \sim \pm 0.02\%$ in comparison with data from Stenflo's team of $\sim \pm 0.002\%$, but nonetheless, the values are in excellent agreement. Again, earlier observations conducted by Stenflo et al. (1983) at a limb distance of $10''$ ($\mu = 0.144$) from the North pole limb produced $p = 0.17\% \pm 0.01\%$, the Glasgow measurements being $p = 0.18\% \pm 0.02\%$.

5. The center-to-limb variation

Unfortunately the pixels of the CCD detector were rectangular so that images recorded at the polar limbs sampled the CLV at a different scale interval relative to images of the equatorial limb. To allow comparison of the various records, it was decided to compare coefficients according to some fitted curve. The semi-analytical expression of Stenflo et al. (1997), viz: $p_{\max} = a(1 - \mu^2)/(\mu + b)$, where μ is the heliocentric angle and a, b are fitted constants, was first tried, but this proved unsuccessful. This equation provides a good representation for optically thin lines but is not applicable to the optically thick H α line whose steep CLV is governed by more complex radiative transfer effects. The chosen empirical expressions followed the form:

$$q = Ae^{(-B\mu)} \quad \text{or} \quad q = Ce^{(-D\alpha)} \quad (7)$$

where μ is the standard heliocentric angle and α is the projected distance from the limb towards the solar centre measured in arcsec; the values of A, C give the peak polarization and B, D describe the decay from the limb towards the solar center. The two forms of equation were considered as their scale sampling relative to the pixel structure is different and it was instructive to investigate the implications of this in relation to the values of the determined parameters (see below). The routine to fit the curves utilised a gradient expansion algorithm to compute non-linear weighted least squares values for the parameter pairs A and B or C and D .

Table 2 provides a sample set of determined coefficients for the three wavelength positions within the H α line at 6562.5\AA (line-core), 6562.2\AA (blue-wing) and 6562.8\AA (red-wing). Both the determined coefficients A and C indicate that the limb polarization is less in the wings of the line than in the line core. This is readily deduced by inspection of Fig. 4 in which the red-wing and line-core CLV are each plotted against the blue-wing variation. It can be seen that the relationship between the the pairs of CLVs is remarkably linear over a large range of μ . The red-wing variation cannot be distinguished from that for the blue-wing with the linear regression passing through the origin with the relationship calculated as $q_r = 0.99q_b$, whereas the line-core values are persistently larger, the linear regression again passing through the origin but with $q_r = 0.79q_c$, the numerical coefficient showing at least a 2σ difference from being unity. The standard deviation of the points around the regression is 0.017 ; the scatter is large, much larger than the observational uncertainties predicted from photon counting statistics and the known instrumental noises. A major observational uncertainty is in the values of μ which, due to the steep CLV of q near the limb leads to a larger scatter relative to the smooth fitted curve. Another source for the scatter may in fact reflect the contribution of solar sources in fact, the chief candidate being the Hanle effect. An example of the effects from this source will be discussed later in a little more detail.

The values of the coefficients of A and C in Table 2 also suggest that, at face value, the polarization at the projected solar pole is marginally higher than at the limb for all three selected

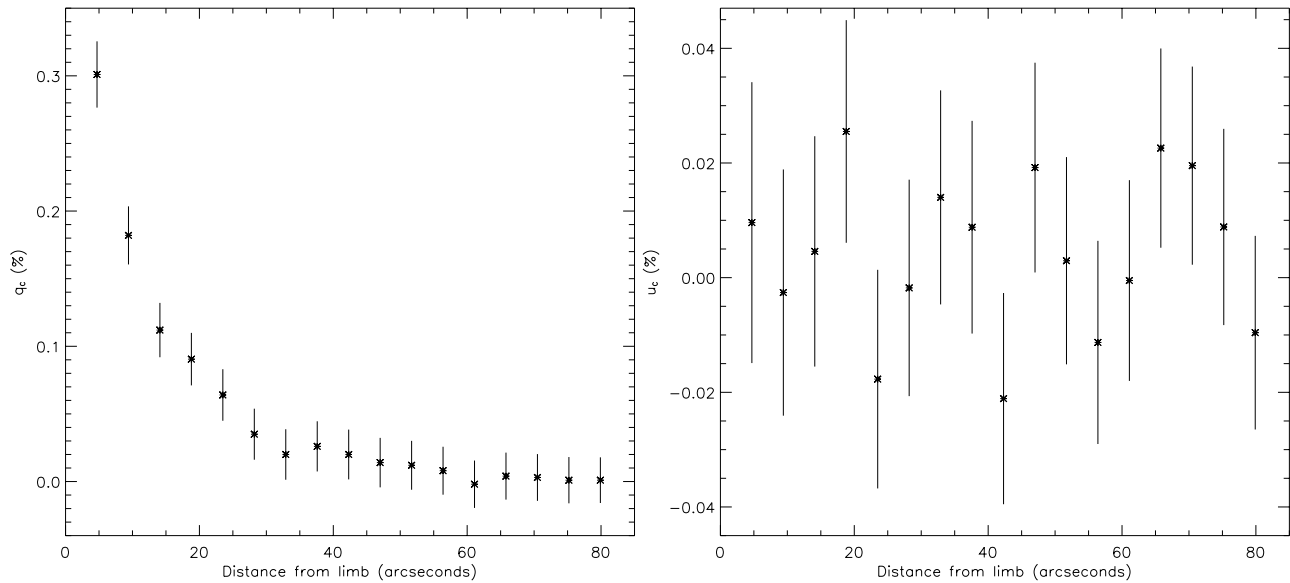


Fig. 3. The northern limb p -CLV of the normalised Stokes parameters, q and u , recorded on 1997 July 19. The monochromator was tuned for the core of the $H\alpha$ line. It may be noted that the q parameter has values $\sim 0.3\%$ at the solar limb with an exponential decay to zero at a limb distance $\sim 60''$; over the same section of the solar limb, the u parameter is essentially zero with recorded values given by the experimental noise.

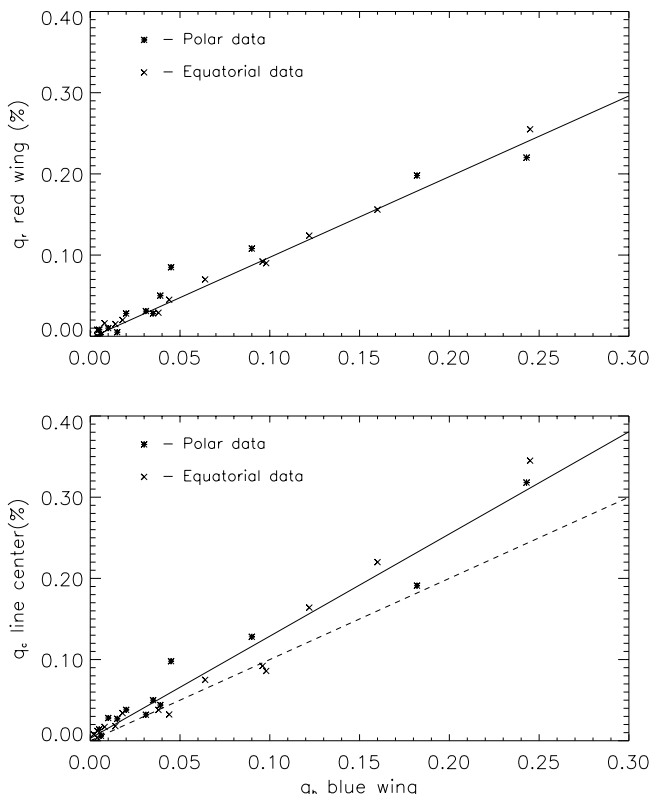


Fig. 4. The upper plot relates the $H\alpha$ red-wing p -CLV to that of the blue-wing. Values from both the solar N Pole and W Limb are included with no distinction being apparent between the two data sets. The lower plot relates the line-core data to those of blue-wing showing that the linear fit (solid line) has a significantly steeper gradient than that for identical variations (dashed line) confirming that, for a given limb distance, p is larger in the line core than in the wing.

Table 2. A sample of fits to data recording the solar CLV of the polarization at $H\alpha$. Measurements on 1997 July 9 were at the core of $H\alpha$ while those for 1997 July 20 were made at the blue- and red-wings of the line; the selected solar region corresponding either to the (North) Pole or (Western) Limb are noted.

Date	$\lambda(\text{\AA})$	Region	A	B	C	D
1997	6562.5	Pole	1.167	13.090	0.485	0.087
Jul 09	Core	Limb	1.154	13.151	0.466	0.084
1997	6562.2	Pole	0.980	13.640	0.380	0.092
Jul 20	Wing	Limb	0.891	13.820	0.352	0.091
1997	6562.8	Pole	0.924	13.226	0.367	0.084
Jul 20	Wing	Limb	0.897	13.219	0.340	0.085

wavelength positions with enhancement ratios of \sim a few percent. Fig. 5 depicts the q polarization measurements for the line-core plotted against μ for both the equatorial and polar limbs with the data trends being indistinguishable by eye. The apparent disparity between the two solar regions may be seen clearly, however, in Fig. 6 in which the center-to-equator values of q are plotted against the centre-to-pole values based on the empirical fits, one for the parameter μ (Fit 1) and the other (Fit 2) for α (see Eq. (7)). For both fits, the gradient appears to be greater than unity, suggesting an enhancement of the polarization produced at the pole relative to that emanating from the equator.

This immediate outcome must be considered with some caution, however. It may be noted that the fitting of data to Eq. (7) depends on its sampling and on any systematic errors associated with the values of μ or α . In the earlier description of the instrument, comment was made on the rectangular shape of the pixels resulting in different spatial sampling rates for

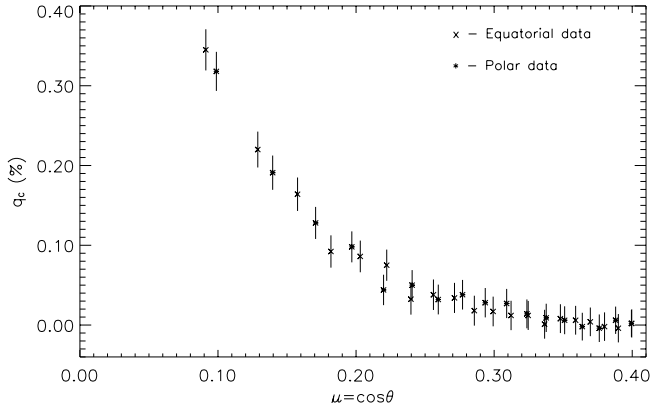


Fig. 5. The measured CLV polar and equatorial q polarization as a function of the heliocentric angle as recorded on 1997 July 9. Error bars (1σ) are indicated for the polarization measurements. The uncertainties on μ are not indicated.

the equatorial and polar regions. Each determined point value represents the signals from pixels which sample the underlying CLV with finite widths, these being different for the pole and equatorial sections; effects of image displacement (whether the limb happens to be placed within a pixel at its center or at its edge) will be different for the two radial sections. In addition, because of the circular shape of the solar image on the rectangular matrix of pixels, the intensity errors introduced by charge transfer inefficiencies at read-out will be different for the polar and equatorial sections. Although the determined values of p for each pixel are not too much affected by this, as each of the four frames is affected in the same way, it does have the effect of altering the apparent scale against which the position of the image is measured. In summary, the CLV can be considered as suffering different convolutions with the pixel strips depending on whether the equator or pole is being measured.

The overall effects outlined immediately above were investigated by shifting the determined polar curve with respect to the equatorial curve along the limb scale and minimising the residual or difference function defined by

$$\Delta = [q(\alpha)_{\text{polar}} - q(\alpha)_{\text{equatorial}}] \quad (8)$$

For the data associated with the line-core, a displacement of the polar curve relative to the equatorial curve by 0.82 arcsec minimised the value of Δ . The application of such a small scale shift, being a fraction of the pixel size sampling interval, is quite acceptable in relation to the local gradients of the CLV and the notion that any recorded pixel signal provides an average value of the CLV over its dimension. With such adjustment, it can be concluded that no significant difference in CLVs can be confidently claimed to exist between the solar pole and its equator to a polarimetric accuracy of about 2 parts in 10^4 . Under the observing conditions pertaining to Glasgow, the spatial resolution of the imaging polarimeter does not exceed $\sim 4''$, and hence the validity of the need for the small corrective factor could not be investigated empirically by shifting the actual solar images and recalculating the q -CLV curves accordingly.

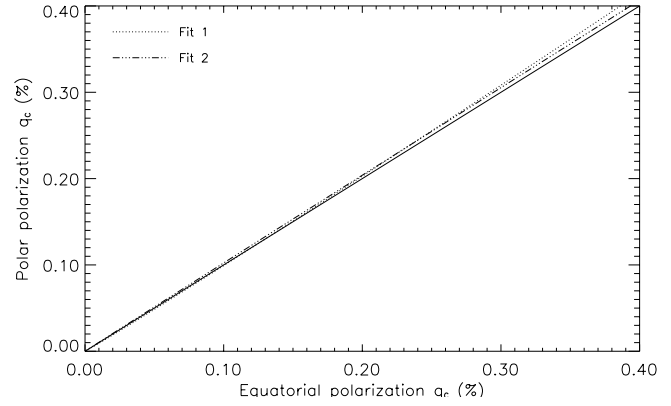


Fig. 6. The center-to-pole q polarization plotted against the center-to-equator q polarization for data recorded on 1997 July 9. The dotted line (Fit 1) corresponds to CLV curves fitted by least squares to the relationship $q = Ae^{-B\mu}$ and the dashed line (Fit 2) corresponds to curves fitted to $q = Ce^{-D\alpha}$. It will be noted that both fits lie above the full line with gradient of unity indicating a polarization at the solar pole that is slightly greater than at the equator.

Similar analyses were conducted for the data for the line-wing data with the same conclusions. Scale shifts ranging between 0.2 to $1''$ were sufficient to remove any statistical significance of disparity in the p -CLV polar and equatorial curves. Thus for all of the data, it can be concluded that no difference of the CLV between the pole and the equator has been detected with polarimetric accuracies $\sim \pm 0.02\%$ or 2 parts in 10^4 and on a spatial resolution $\sim 1''$, the latter figure being the maximum value of scale shift required to remove the face value disparities as indicated in Table 2.

A further possible problem associated with any comparison of the CLV of E/W and N/S sections of the solar photosphere is the influence of refraction by the Earth's atmosphere. For measurements made along the N/S direction, the solar image is compressed by differential refraction making the underlying CLV gradient seem steeper than for the undistorted E/W direction. With the embedded linear scale of the instrument, this means that at some apparent position from the limb, the polarization on a N/S radius will appear to be less than for an equivalent position along an E/W radius.

The scale of differential refraction can be estimated by considering the refraction, R in arcsec, to be approximated by $R = k \tan \zeta$, where $k \sim 60''$ and ζ is the zenith distance. Using this formula, simple calculation shows that at a zenith distance of 50° , a $10'$ strip along the N/S direction encompasses an additional $1''$ of the solar photosphere, i.e. the CLV baseline is compressed by about 1 part in 600. In terms of the field of view of a pixel, any compaction of the recorded CLV is too small to become apparent and would be masked by the pixel/sampling problem outlined above. In any case, the apparent increase of the level of the polar CLV relative to that of the equator has the wrong sense as to what differential refraction predicts. It may be mentioned that although the sense is right to explain the disparity of polar/equator CLV comparisons reported by Leroy (1972) at 3800\AA , even allowing for the increase in value of k for

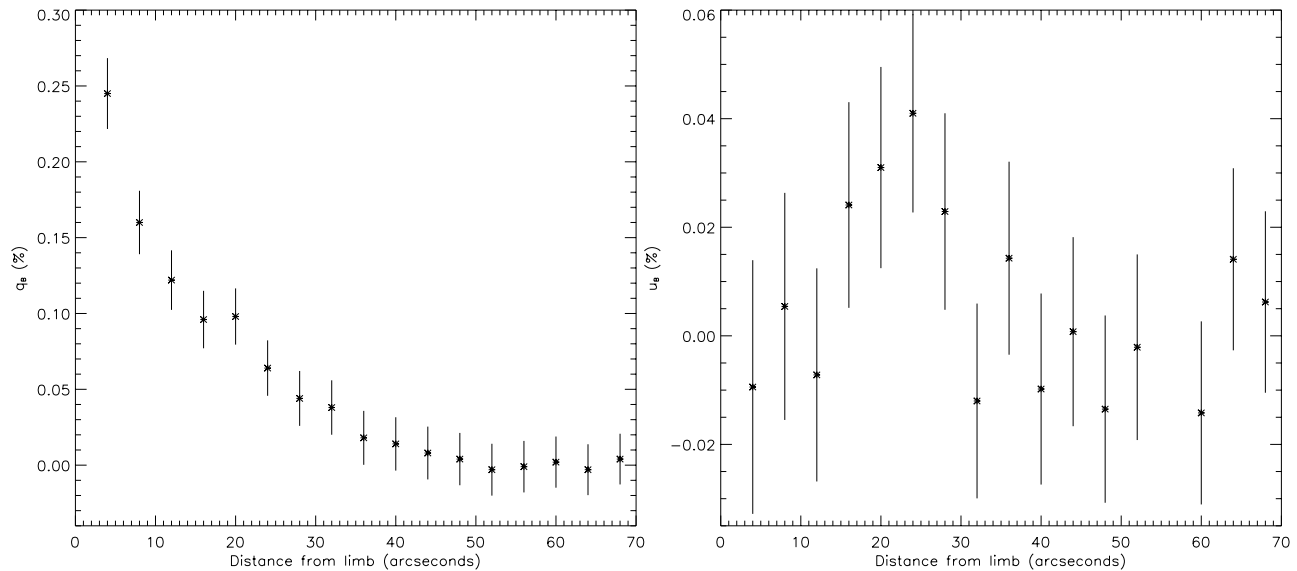


Fig. 7. The CLV data for measurements for 1997 July 20 at the Western limb in the H α blue-wing are plotted for both q and u . At a limb distance of 20 arcsec, the q value appears to deviate at low significance from the underlying curve. At the same value of μ , the u value departs significantly from zero. Similar variations were apparent at the H α red-wing position but unfortunately observations at the line core were not made at the time to see the likely enhancement of the effect at this wavelength position.

this wavelength, its scale still appears to be too small to provide a satisfactory explanation for his result.

6. The Hanle effect

It was mentioned earlier that some recorded CLVs occasionally exhibited deviations from the fitted smooth curve, with their origin ascribable to solar sources. An example of this behaviour is illustrated in Fig. 7 for 1997 July 20 for the record of the solar Western limb in the blue-wing of H α . Inside the limb, at about 20 arcsec, the q value is raised marginally with respect to the fitted CLV curve. By itself, this departure is barely statistically significant but it may be noted that the u parameter departs from zero at the same location, indicating that the position angle of the polarization suffers a rotation $\sim 8^\circ$ with respect to the radius vector, it being remembered that $\tan 2\theta = u/q$. A similar behaviour was also recorded for the red-wing position within the H α line.

Such a rotation of the polarization vector is systematic of the Hanle effect, associated with resonance scattering in the presence of a weak magnetic field. It may be noted, however, that p is slightly enhanced in this region with the basic Hanle effect predicting a depolarization (for example, see Stenflo, et al., 1998). In the case of this feature as observed within the H α line, the underlying polarization must already have been enhanced by effects associated with a local variation in the optical depth, prior to the influence of the Hanle mechanism.

7. Conclusion

A simple imaging polarimeter has been designed and constructed for investigating the center-to-limb variations of the solar polarization within the H α line. Spectral resolution is

achieved by a narrow-band interference filter with sufficient throughput to maintain the position of its central passband to within its spectral resolution ($\Delta\lambda = 0.4\text{\AA}$) over a field of view $\sim 10'$. By using pairs of images corresponding to the orthogonal polarizations, values of p can be mapped with both the effects of variable atmospheric transmission and of unequal pixel sensitivities removed. By recording the data via a CCD system, a set of frames corresponding to four settings of the polarimetric modulator provides values of p with 1σ accuracies $\sim \Delta p = \pm 0.0002$ or $\pm 0.02\%$ per pixel.

Measurements made of the Sun at the Glasgow University Observatory of the CLV at H α reveal that, in this line, the degree of polarization is larger than the nearby continuum, the enhancement arising from resonant scattering effects. Departures from smooth CLVs are also detectable, these being relatable to the Hanle effect.

The immediate reduced p values determined for the solar pole and the equator suggest that the former displays larger polarizations. The disparity is not thought to originate in the Sun, however, and is reconciled by adjusting the fiducials for the solar limb position. The need for the corrections is explainable in terms of the rectangular shape of the CCD pixels and the difference of their orientation with respect to the radius vectors associated with the polar and equatorial sections. A shift by a small fraction of the size of a pixel removes the apparent polarization disparities to the limit of the measurement accuracies of $\Delta p = \pm 0.0002$ and to a spatial resolution of $\sim 1''$. It may be concluded, therefore, that at these experimental limits, no polarizational differences have been detected at the H α line between the solar poles and the equator.

If it is desired to improve on these solar polarimetric experiments, say with a view to correlating p -CLV with the solar

chromospheric prolateness as measured purely by photometry by Auchère et al. (1998), it would be useful to construct an instrument with a larger plate scale and to use a CCD with smaller and square pixels.

Acknowledgements. We wish to thank Colin Hunter at the Observatory Workshop for the fabrication of the instrument and for support during the observations. This work was carried out under a Rolling Grant from PPARC and VA received support under a PPARC CASE award.

References

- Ameijenda V., 1998, Ph.D. Thesis – Dept of Physics & Astron., Univ. of Glasgow
- Auchère F., Boulade S., Koutchmy S., et al., 1998, A&A 336, L57
- Bianda M., Solanki S.K., Stenflo J.O., 1998a, A&A 331, 760
- Bianda M., Stenflo J.O., Solanki S.K., 1998b, A&A 337, 565
- Billings B.H., 1951, JOSA 41, 966
- Clarke D., Fullerton S.R., 1996, A&A 310, 331
- Clarke D., Grainger J.F., 1971, Polarized Light and Optical Measurement. Pergamon Press, Oxford
- Dollfus A., 1974, In: Gehrels T. (ed.) Planets, Stars and Nebulae Studied with Photopolarimetry. Univ. Arizona Press, p. 695
- Dumont S., Pecker J.C., 1971, A&A 10, 118
- Keller C.U., 1998, Private Communication
- Leroy J.-F., 1972, A&A 19, 287
- Mickey D.L., Orrall F.Q., 1974, A&A 31, 179
- Öhman Y., 1939, MNRAS 99, 624
- Pickering E.C., 1873, Am. Acad. of Arts and Science 9, 1
- Pospergelis M.M., 1965, SvA 9, 313
- Scarrott S.M., 1983, MNRAS 204, 1163
- Scarrott S.M., 1991, Vistas in Astronomy 34, 163
- Stenflo J.O., 1996, Solar Physics 164, 1
- Stenflo J.O., Keller C.U., 1997, A&A 321, 927
- Stenflo J.O., Twerenbold D., Harvey J.W., et al., 1983, A&AS 54, 505
- Stenflo J.O., Bianda M., Keller C.U., et al., 1997, A&A 322, 985
- Stenflo J.O., Keller C.U., Gandorfer A., 1998, A&A 329, 319
- Tinbergen J., 1996, Astronomical Polarimetry. Cambridge Univ. Press